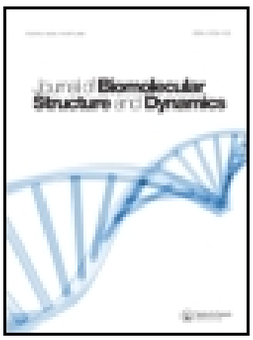

Taylor & Francis
Taylor & Francis Group

Journal of Biomolecular Structure and Dynamics

ISSN: 0739-1102 (Print) 1538-0254 (Online) Journal homepage: https://www.tandfonline.com/loi/tbsd20

Design potential selective inhibitors for human leukocyte common antigen-related (PTP-LAR) with fragment replace approach

Jing-Wei Wu, Huan Zhang, Wei-Ya Li, Xue Tang, Hong-Lian Li, Xin-Hua Lu, Zhi-Hui Zheng, Ying Ma & Run-Ling Wang

To cite this article: Jing-Wei Wu, Huan Zhang, Wei-Ya Li, Xue Tang, Hong-Lian Li, Xin-Hua Lu, Zhi-Hui Zheng, Ying Ma & Run-Ling Wang (2019): Design potential selective inhibitors for human leukocyte common antigen-related (PTP-LAR) with fragment replace approach, Journal of Biomolecular Structure and Dynamics, DOI: 10.1080/07391102.2019.1699862

To link to this article: https://doi.org/10.1080/07391102.2019.1699862

Design potential selective inhibitors for human leukocyte common antigen-related (PTP-LAR) with fragment replace approach

Jing-Wei Wu[a,1], Huan Zhang [b,1], Wei-Ya Li[a,1],Xue Tang[c], Hong-Lian Li[a], Xin-Hua Lu[d], Zhi-Hui Zheng[d], Ying Ma[a,*], Run-Ling Wang[a,*]

[a]Tianjin Key Laboratory on Technologies Enabling Development of Clinical Therapeutics and Diagnostics (Theranostics), School of Pharmacy, Tianjin Medical University, Tianjin 300070, China; Tel/Fax: +86-22-83336690;

[b]Department of Pharmacy, Tianjin Medical University General Hospital, Tianjin 300052, China; Tel/Fax: +86-22-60362235;

[c]Tasly Research Institute, Tasly Holding Group Co., Ltd, Tianjin

[d]New Drug Research and Development Center of North China Pharmaceutical Group Corporation, National Microbial Medicine Engineering and Research Center, Hebei Industry Microbial Metabolic Engineering &Technology Research Center, Key Laboratory for New Drug Screening Technology of Shijiazhuang City, Shijiazhuang, Hebei, China.

[1] These authors contributed equally to this work;

[*]Corresponding author. Email-address: maying@tmu.edu.cn (Y Ma); wangrunling@tmu.edu.cn (R.-L. Wang).

Abstract

The overexpression of PTP-LAR could cause the insulin resistance, so PTP-LAR might be a promising target for treating diabetes. In this study, we applied the computer modeling methods with fragment replace approach to screen the fragment database by targeting PTP

domain and site B with the aim to discover potent and selective PTP-LAR inhibitors. A series of novel 4-thiazolidone derivatives were gained. The results of their ADMET predictions indicated that these new compounds might become drug candidates. The series of these derivatives were synthesized. Subsequently, their PTP-LAR inhibitory activities were assayed. The compound7d showed highly selectivity for PTP-LAR (10.41 μM) over its close homolog PTP1B (IC_{50}=44.40 μM), SHP2 (IC_{50}>122.81 μM) and CDC25B (IC_{50}>122.81 μM) and docking and molecular dynamics simulation were applied to propose the most likely binding mode of compound7d with PTP-LAR. Thus, our findings reported here may pave a way for discovering potential selective PTP-LAR inhibitors.

Keywords: PTP-LAR; fragment replace; synthesis; docking; molecular dynamics

Abbreviations: PTP-LAR, Human leukocyte common antigen-related; PTP, Protein Tyrosine Phosphatase; IR, insulin receptor; PTP1B, Protein tyrosine phosphatase-1B; LRP, Lung resistance protein; ADMET, absorption, distribution, metabolism, excretion, toxicity; PPB, plasma protein binding; BBB, blood brain barrier penetration; CYP450, cytochrome P450; HIA, human intestinal absorption; TLC, thin-layer chromatography; UV, Ultra Violet; NMR, nuclear magnetic resonance; TMS, tetramethylsilane; MS, mass spectrometry; ANM, anisotropic network mode; PDB, Protein Data Bank; DMF, N,N-Dimethylformamide; pNPP, para-nitrophenyl phosphate; DTT, dithiothreitol; MD, molecular dynamic; RMSD, root-mean-square deviation; RMSF, root-mean-square fluctuation; SPC, single-point charge; PME, Particle Mesh Ewald; MM-PBSA, molecular mechanics Poisson Boltzmann surface area; H bond, hydrogen bond; VDW, Van der Waals.

Introduction

Diabetes, a group of metabolic disease, is characterized by high blood sugar levels for a long period either resulting from the pancreas could not produce enough insulin, or resulting

from the cells of the body are not responding properly to the insulin produced(Roper, Spinderella & Webb 2014). It is classified into three main types: diabetes mellitus type 1(Michigan Dental 2007); diabetes mellitus, type 2(Mediavilla Bravo 2014); Gestational diabetes, which is one of the most common and life threatening chronic diseases and becomes the biggest killer in India, China, and Brazil(Viswanathan & Sathyamurthy 2015; Zhu & Zhang 2016). The prevalence of diabetes for the individuals in the worldwide was estimated to be 4.4% in 2030 and nearly 1.5 to 5.0 million people will dead each year because of the diabetes (Rathmann & Giani 2004; Wild, Roglic, Green, Sicree & King 2004). Therefore, it is the most pressing task to discover novel target for treating diabetes for these suffering patients. Human leukocyte common antigen-related (PTP-LAR), a receptor-like classical transmembrane phosphatase, has received considerable attentions for developing novel and effective agents for treating diabetes (Elchebly, Cheng & Tremblay 2000; Chagnon, Uetani & Tremblay 2004; Xu, Schwab & Marette 2014).

PTP-LAR, a member of the family of the receptor type IIA PTPs, regulates multiple receptor tyrosine kinases, in turn, would control insulin receptor signaling and glucose homeostasis(Chagnon, Uetani & Tremblay 2004; Ajay & Sobhia 2012). The PTP-LAR is composed of two structures, namely extracellular structure and intracellular structure. Both the membrane proximal PTP domain (D1) and a membrane distal PTP domain (D2) in the intracellular structure were capable of catalytic activity.(Pulido, Serra-Pages, Tang & Streuli 1995). It is expressed in the plasma membrane of insulin-sensitive cells which plays a vital role in dephosphorylation insulin receptor (Hashimoto, Feener, Zhang & Goldstein 1992; Zhang, Li, Oswald & Goldstein 1996). The inhibition of PTP-LAR by 63% in the rat McA-RH7777 hepatoma cell line caused 3-4 fold increases in insulin receptor signaling(Kulas, Zhang, Goldstein, Furlanetto & Mooney 1995). Experimental evidences show that PTP-LAR could decrease IR autophosphorylation and kinase activity by 47% (Ahmad & Goldstein 1997). When compared with PTP1B and LRP, LAR preferentially dephosphorylated the IR Tyr-1150 domain-a vital residue to the IR activity, which is 3.5 and 3.7 times more rapidly than PTP1B and LRP, respectively(Hashimoto et al. 1992). The LAR-PTP D1 domain plays

an important role in dephosphorylation of tyrosine-phosphorylated IR(Tsujikawa et al. 2001). Zabolotny lab discovered that transgenic mice with the overexpress human PTP-LAR caused the fasting plasma insulin increased 2.5 fold in muscle and the whole-body glucose disposal and glucose uptake into muscle were reduced by 39–50%, leading to the insulin resistance(Zabolotny et al. 2001). The PTP-LAR (-/-) mice in the fast state showed the heightened level of insulin sensitivity which is characterized by lower plasma insulin and the reduction rate of hepatic glucose production (Ren et al. 1998). Therefore, PTP-LAR inhibitors have caught substantial attention for developing powerful drugs against diabetes.

However, there is great challenge to find selective PTP-LAR inhibitors for two reasons : firstly, there is no crystal complex structure of the PTP-LAR and the ligand; secondly, highly homology in all PTPs with structural conservation-HCXAGXXR in the PTP catalytic domain (Guan & Dixon 1991). In this study, fragment replace approach was applied to screen the fragment database in order to discover selective PTP-LAR inhibitors, as well as the molecular dynamic simulation was used to analyze the binding interactions between PTP-LAR and the inhibitors. Hopefully, the findings found here may pave the way to discover the selective PTP-LAR inhibitors to treat diabetes and the inhibitors may act as a tool to understand the PTP-LAR's complex signal transduction cascades.

Materials and Methods

Virtual screening

The receptor crystal structure of PTP-LAR (PDB ID: 1LAR) was chosen for modeling(Berman et al. 2002). The reasons for selecting the protein are that: (1) the resolution of the crystal structure is 2.0 Å; (2) the source organism of the structure was humans(Nam, Poy, Krueger, Saito & Frederick 1999). All the protocol used in virtual screening was embedded in the Discovery studio v3.5.

Prepare protein protocol was utilized to prepare protein including the operations of the cleaning the protein, optimizing side-chain conformation for residues, removing water molecules, predicting titration site pKs and protonating the structure at the specified pH of

7.0±2.0, and adding hydrogen, as well as minimizing energy using the CHARMm minimization procedure(MacKerell, Banavali & Foloppe 2001). Meanwhile, the ligand preparation consisted of enumerating valid ionization states at the specified pH of 7.0 ± 2.0, tautomers, isomers, fixing bad valencies, and generating a reasonable 3D conformation using Catalyst by the Prepare Ligands protocol(Andrew S. 1995; Andrew S. 1995; Andrew S. 1995). In this study, there is no-crystallized ligand, thus we have implemented a binding site definition tool to define the binding pocket. Active site pocket residues of PTP-LAR contains the pTyr recognition loop (residues 1352-1355), WPD-loop (residues 1488-1490), P-loop (residues 1521-1528). A sphere was created around the binding site residues with the 15 Å radius adjusted to include them. Virtual screening was carried out by the LibDock tool. Molecular docking of the ligands to the PTP-LAR receptor was carried out in the current study by using CDOCKER.

Owing to the crystal of 1LAR with no crystal ligand, the validation was done by using the linear regression analysis method prior to virtual screening. 20 PTP-LAR inhibitors were docked into the binding sites, respectively. The correlation coefficient was calculated between dock score and the pIC_{50}.

In order to discover the potential hit compounds for PTP-LAR, approximately 50, 000 compounds selected from ZINC druglike database were utilized in the docking-based virtual screening.

Molecular Docking with Fragment Replace Method

In this study, Fragment Replace embedded in the Discovery studio v 3.5 was employed to replace the fragment and perform the molecular docking. Fragment Replace is a very powerful technique for new drug design because it often used to improve the ADMET profile to help overcome unwanted properties or to improve potency or selectivity toward the target protein by generating new lead compounds with improved core properties(Premnath et al. 2014; Wu, Sun, Zhou, Ma & Wang 2019).

The procedures of the scaffold hopping to identify replacement fragments can be briefly

described as follows. Firstly, the receptor grid file and other interacting_residues group were defined, which not only allowed the steric restraint of the protein active site to refine the novel ligands generated and but also allowed the replacement fragments to interact with any one of the residues defined in the interacting_residues group. Secondly, the fragment was defined to replace. Thirdly, the fragment libraries which were derived from ZINC were defined (Irwin & Shoichet 2005). Fourthly, suitable fragments were discovered to fit the receptor cavity. Finally, the fragments were attached to the core. The novel ligands are sorted and filtered by a parato sort, including the interactions formed with the protein, Lipinski violations(Walters 2012; Lipinski 2016), receptor bumps, and fragment "novelty". After all the above steps were finished, all the compounds gained from the Fragment Replace were redocked into the receptor pocket through the rigid protein docking model with the CHARMm energy to estimate the binding affinities.

ADMET Prediction

Absorption, distribution, metabolism,excretion and toxicity (ADMET)(Lombardo, Gifford & Shalaeva 2003) properties are a crucial aspect of clinical candidate quality. Approximately 39% of drugs were failing in development because of poor biopharmaceutical properties. Lipinski's rule of five (Lipinski, Lombardo, Dominy & Feeney 2001) is a rule of thumb to evaluate druglikeness or determine if a chemical compound would become a likely orally active drug in humans. Incorporating ADMET predictions play an important role in the drug development process, which could thus generate lead compounds that are more likely to satisfy the Lipinski's rule of five during clinical trials.

In present work, we adopted the program of ADMET embedded in the Discovery studio v3.5 which is an accurate program for predicting the ADMET properties of the compounds. All the investigated compounds need to be prepared before using ADMET program. The preparation consisted of enumerating valid ionization states at the specified pH of 7.0, tautomers, isomers, fixing bad valencies, and generating a reasonable 3D conformation. The property analysis for log P, the aqueous solubility(Cheng & Merz 2003), blood brain barrier

penetration (BBB)(Egan, Walters & Murcko 2002), cytochrome P450 (CYP450) 2D6 inhibition(Wesson & Eisenberg 1992; Susnow & Dixon 2003), hepatotoxicity(Cheng & Dixon 2003; Xia, Maliski, Gallant & Rogers 2004), human intestinal absorption (HIA)(Egan, Merz & Baldwin 2000; Egan & Lauri 2002), plasma protein binding(Dixon & Merz 2001; Votano et al. 2006) and PSA was computed in the ADMET program to evaluate whether the compounds hold the potential to become drug candidates.

Chemistry

All the reagents were obtained from commercial suppliers and were used without further purification. All the reactions were monitored by thin-layer chromatography (TLC) on silica gel precoated F254 Merck plates, and spots were examined under UV light (254 nm). All column chromatography was performed using 200-300 mesh silica gel. ^{1}H NMR was taken on a Bruker Avance 400-MHz NMR Spectrometer at 300 K with TMS as the internal standard, and $CDCl_3$ was used as solvent. MS spectra were recorded on an Agilent 1100 LC/MSD (ESI) Mass Spectrum.

PTP Activity Assay

Human recombinant PTP-LAR, PTP1B, SHP2 and CDC25B were expressed in E. coli (BL21) and purified by Glutathione Sepharose 4B affinity chromatography. pNPP(para-nitrophenyl phosphate) was used as phosphatase substrate. Firstly, purified recombinant PTP-LAR, PTP1B, SHP2 and CDC25B (0.05 μg) in 50 μL buffer with 50 mM citrate (pH 6.0), 0.1 M NaCl, 1 mM EDTA, and 1 mM dithiothreitol (DTT) and test compounds were added to each well of a 96-well plate to preincubate for 15 min at room temperature. Blank was prepared by omitting enzyme and substituting an equivalent volume of buffer. Secondly, 50 μL of reaction buffer with 10 mM pNPP was added and incubated at 37 °C for 30 min. Thirdly, the reaction was stopped by adding 10 μL 0.2 M sodium hydroxide and chilled on ice quickly. Finally, the amount of pNP was measured by detecting the absorption at 405 nm against blank. The positive control used in the enzymatic assay is sodium orthovanadate. The

IC_{50} values were determined by analyzing the data using ORIGINPRO 8 software.

Molecular Dynamics

The "GROMACS 4.5.5 package" (Hess, Kutzner, van der Spoel & Lindahl 2008)was adopted to study the internal motions of the receptor-ligand system. The interactions of LAR with the best hit identified from screening of "Replace Fragment" were investigated through MD simulation using GROMACS 4.5.5 package with GROMACS 43a1 force field(Pol-Fachin, Fernandes & Verli 2009) for 50 ns. The topology files and charges for the ligand atoms were generated using the PRODRG 4.0 Server(van Aalten et al. 1996). All the models were simulated by incorporating space-filling cubic boxes which are filled with explicit single-point charge (SPC) water molecules. The models were covered with a water shell of 1.0 nm from the surface of the protein. The system was neutralized and equilibrated with counter ions to replace SPC water molecules randomly. Subsequently, the models were minimized using steepest descent approach(Ftanik & Horvath 1989). NPT and NVT canonical ensemble (N= number of partical, P= system pressure, V= volume, and T= temperature)-based calculations were performed for keeping the temperature at 310 K and pressure at 1 atm using Berendsen coupling algorithm. The Particle Mesh Ewald algorithm(Konerding, Cheatham, Kollman & James 1999; Norberto de Souza & Ornstein 1999) was used to calculate the electrostatic interactions. All bonds were constrained by using the LINCS algorithm(Hess 2008). Both the Van der Waals and Coulomb interactions were truncated at 1.2 nm.

Results and discussion

Virtual screening and molecular docking with Fragment Replace method

Active site pocket residues of PTP-LAR contains the pTyr recognition loop (residues 1352-1355), WPD-loop (residues 1488-1490), P-loop (residues 1521-1528).The site B is non-catalytic phosphate binding site, which is unique to PTP-LAR and contains hydrophobic residues for potential nonpolar interactions (Asn1357, and Tyr1563)(Nam et al. 1999). Owing

to the crystals of PTP-LAR-1LAR without crystal ligands, its validation was done by using the linear regression analysis method. 20 reported PTP-LAR inhibitors were docked into the binding sites. The correlation coefficient was calculated between the pIC_{50} and the docking score. The acceptable correlation coefficients of 0.93(PTP-LAR) was obtained, indicating that the binding model is reliable (Figure S1). Encouraged by the aforementioned studies, it should be possible to develop compounds that can not only simultaneously occupy active sites to gain higher affinity but also target the site B to improve the selectivity. The detailed procedure of discovering the desired selective inhibitors is shown in Figure 1. At the first stage, the lead compound database, one subdatabase of the ZINC(Irwin & Shoichet 2005), was screened by utilizing the LibDock tool embedded in Discovery Studio v3.5 for its optimal performance targeting the PTP-LAR. The top hit-ZINC33404314, a 4-thiazolidone scaffold was selected as the optimal lead compound for further modification, because the oxygen of the –C=O of 4-thiazolidone ring can form hydrogen bonding with Lys 1433, and two more H-bond formed by the oxygen atom of the carboxylic acid to the residues of Trp1488 and Gln1570, respectively. The carboxylic acid would cause gastric irritation in sensitive persons. Consequently, the carboxylic acid group in ZINC33404314 is modified into ethyl ester group. Subsequently, the Fragment Replace method was used to search the fragment database for the desired chemical groups to attach to the template. This was to help lengthen the 4-thiazolidone ring structure to make it better fit the roomy space in site B to improve selectivity of other PTPase. After that, each of the derivative compounds was docked into the two receptors PTP-LAR (1LAR), PTP1B (2VEW), SHP2 (2SHP) and CDC25B (PDB ID: 1CWT) respectively. Subsequently, a series of compound candidates modified from the 4-thiazolidone ring structure were generated, and then, the top eight compounds with the best binding score computed by CDOCKER program are listed in Figure 1. As a result, the hydrogen circled by purple circle of comp#0 in Figure 1 was replaced by the linker groups colored in green. The best groups (i.e., Ar1 and Ar2) were added to the template.

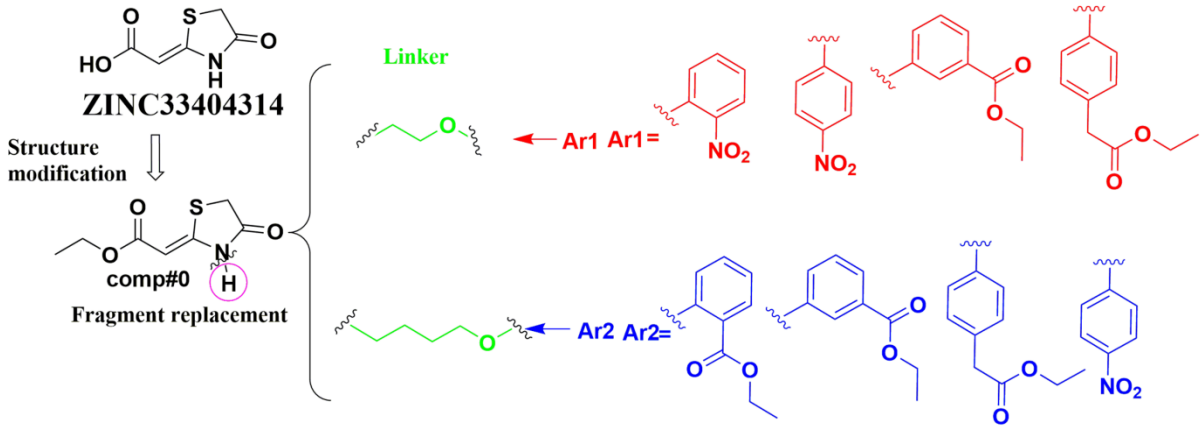

Figure 1: Generation of the 8 derivative compounds from 4-thiazolidone ring by core hopping method.

ADMET

There are two key factors that affect oral bioavailability: One is solubility, the other is

	ALogP[a]	Solubility-level[b]	BBB-Level[c]	CYP2D6 Prediction	Hepatotoxic# Prediction	Absorption -level[d]	PPB# Prediction	PSA_2D
7a	3.172	3	2	False	False	0	True	82.045
7b	2.529	3	3	False	False	0	True	82.045
7c	3.172	3	2	False	False	0	True	82.045
7d	2.529	3	3	False	False	0	True	82.045
7e	3.207	3	2	False	False	0	True	82.045
7f	0.91	4	3	False	False	0	True	102.152
7g	1.552	4	3	False	False	0	True	102.152
7h	0.91	4	3	False	True	0	True	102.152

Human Intestinal Absorption (HIA). Solubility plays an important role in the pharmacological activity of a compound. HIA has a pronounced affect on the therapeutic effect of drugs. All compounds showed good human intestinal absorption due to appropriate LogP and Aqueous solubility. Plasma protein plays a vital role in drug distribution. All compounds were found to be highly bound with plasma protein. CYP2D6 is one of the important enzymes involved in drug metabolism, which is responsible for the metabolism and

elimination of approximately 25% of clinically used drugs. Eight compounds were predicted to be non-inhibitors of cytochrome P450 2D6 (CYP2D6). For hepatotoxicity, seven compounds were predicted non-toxic. For brain/blood barrier, compound 7a, 7c, 7e had a moderate penetrant level, and the other five compounds showed a poor penetrant level. Therefore, as mentioned above, the values for the ADMET properties of all compounds except compound7h listed in Table 1 are within the acceptable range for human beings, indicating these compounds found in this study can be utilized as candidates for the purpose of developing new drugs.

Table 1 the ADMET prediction for the 4-thiazolidone derivatives.

a:AlogP, the logarithm of the partition coefficient between n-octanol and water; b:Aqueous solubility level: 0 (extremely low); 1 (very low, but possible); 2 (low); 3 (good);4(optimal);c: BBB level: 0 (very good); 1 (good); 2 (moderate); 3 (poor);4(undefined) ; d: Human intestinal absorption level: 0 (good); 1 (moderate); 2 (poor); 3 (very poor).

Chemistry

The synthetic routes of all the 8 target compounds were shown in Schemes 1. As shown in Scheme 1, ethyl 2-cyanoacetate was reacted with ethyl 2-mercaptoacetate using K_2CO_3 as the catalyst to produce compound3. Esterification of hydroxybenzoic acid(compound 4a-c) with EtOH in the presence of $SOCl_2$ at reflux smoothly afforded compound 4a-c. The hydroxybenzoate (compound 5a-c) or nitrophenol(compound 5d-e) was reacted with 1,2-dibromoethane or 1,4-dibromobutane to afford phenolic ether (compound 6a-h), which were further reacted with compound3 to give the final compound 7a-h using K_2CO_3 as the catalyst by nucleophilic substitution reaction(Markovic, Baranac, Dzambaski, Stojanovic & Steel 2003; Markovic, Pergal, Baranac, Stanisavljev & Stojanovic 2006; Wu et al. 2019).

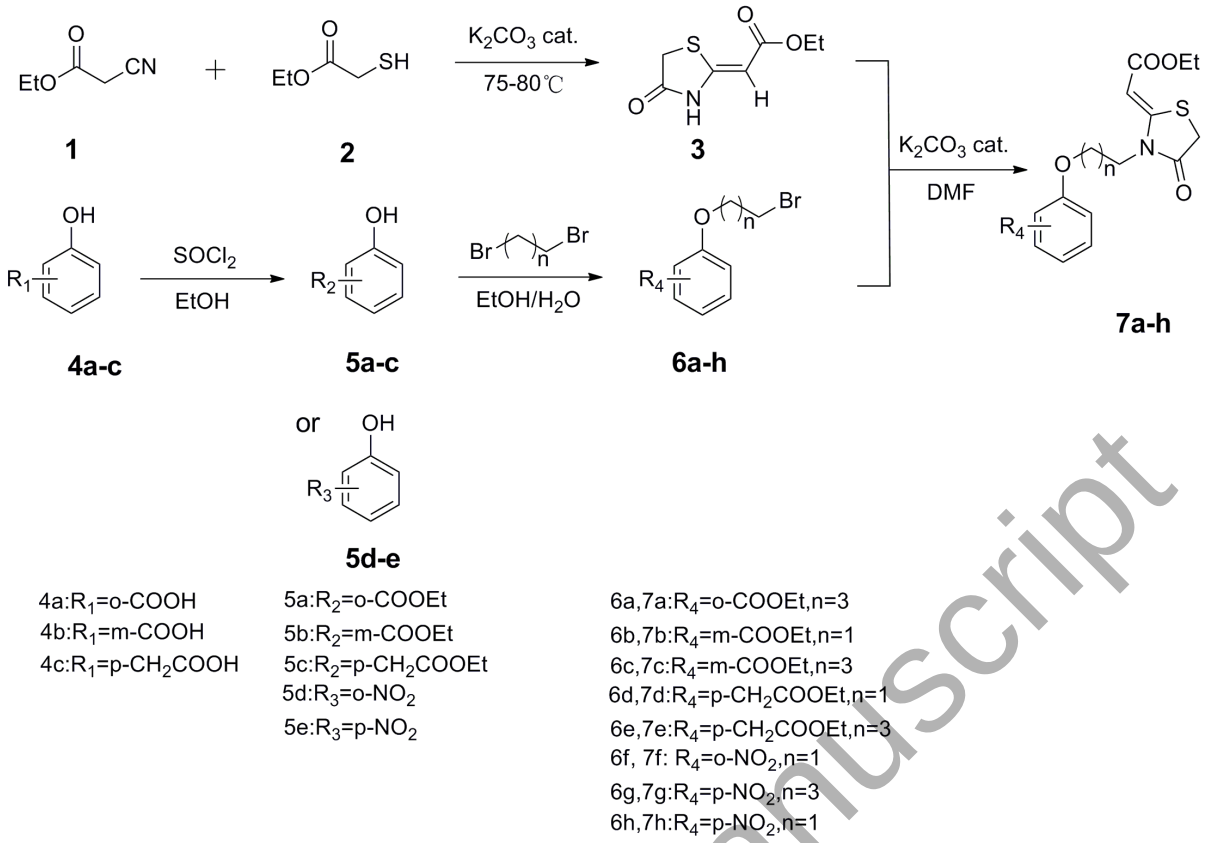

4a:R_1=o-COOH
4b:R_1=m-COOH
4c:R_1=p-CH_2COOH

5a:R_2=o-COOEt
5b:R_2=m-COOEt
5c:R_2=p-CH_2COOEt
5d:R_3=o-NO_2
5e:R_3=p-NO_2

6a,7a:R_4=o-COOEt,n=3
6b,7b:R_4=m-COOEt,n=1
6c,7c:R_4=m-COOEt,n=3
6d,7d:R_4=p-CH_2COOEt,n=1
6e,7e:R_4=p-CH_2COOEt,n=3
6f, 7f: R_4=o-NO_2,n=1
6g,7g:R_4=p-NO_2,n=3
6h,7h:R_4=p-NO_2,n=1

Scheme 1: Synthesis of compound7a-7h.

General procedure for the synthesis of 7a-7h.

A mixture of ethyl 2-isocyanoacetate (50 mmol) and K_2CO_3 (2.5 mmol) was stirred at room temperature for 10 min. The ethyl 2-mercaptoacetate (52.5 mmol) was then added into the mixture. The result mixture was heated at reflux for 50 min, cooled to the room temperature. Then water and ethanol 7：3(v/v) (70 mL) were added to the mixture. Then, the mixture was stirred for 1 h and filtrated to afford compound3, 9.63 g (yield 95.7%).

To a solution of hydroxybenzoic acid (compound 4a or compound 4b or compound 4c) (20 mmol) in EtOH (200 mL) at room temperature, was added $SOCl_2$ (40 mmol) in dropwise at 0 ^{O}C. The mixture was stirred for 1 hour at room temperature slowly and heated at reflux for 8 h, cooled to room temperature. The solvent was removed by rotary evaporation. The residue was dissolved in 50 mL of ethyl acetate. The mixture was washed with water and brine and dried over anhydrous Na_2SO_4, and concentrated *in vacuo*. Then, the crude

compound 5a-c was used without further purification.

A mixture of compound 5a (or compound 5b or compound 5c or compound 5d or compound 5e) (10 mmol), ethyl 2-bromoacetate (20 mmol), K_2CO_3 (20 mmol) and EtOH (20 mL) was refluxed for 24 h. TLC showed that there was no compound 5a (or compound 5b or compound 5c or compound 5d or compound 5e). After removal of solvent, the residue was dissolved in ethyl acetate (150 mL), and washed with water and saturated brines, dried over $MgSO_4$ and concentrated *in vacuo*. The residue was purified by column chromatography on 200–300 mesh silica gel with petroleum ether: ethyl acetate= 7:1to give product compound 6a-h.

A mixture of compound 6a (or compound 6b, or compound 6c, or compound 6d , or compound 6e, or compound 6f, or compound 6g, or compound 6h) (3.6 mmol), K_2CO_3 (6 mmol), KI (0.3 mmol), and compound3 (3.0 mmol）) in DMF (20 mL) was stirred at room temperature for 5 h. After removal of solvent, the residue was dissolved in ethyl acetate (150 mL) and washed with brine and dried over anhydrous $MgSO_4$, and concentrated *in vacuo*, the residual was purified by column chromatography on 200–300 mesh silica gel with petroleum ether: ethyl acetate= 1:1to give product compound 7a-h.

ethyl(Z)-2-(4-(2-(2-ethoxy-2-oxoethylidene)-4-oxothiazolidin-3-yl)butoxy)benzoate (compound 7a)

^{1}H-NMR(CDCl3,400MHz): δ: 7.80 (d, 2H, J = 8.4 Hz), 7.43 (d, 2H, J = 8.4 Hz), 7.00 (t, 1H, J = 7.8 Hz), 6.93 (t, 1H, J = 8.0 Hz), 5.53 (s, 1H), 4.36 (q, 2H, J = 7.2 Hz), 4.31 (q, 2H, J = 7.2 Hz), 4.20 (t, 2H, J = 5.4 Hz), 3.80 (t, 2H, J = 4.2 Hz), 3.70 (s, 2H), 1.35-1.38 (m, 4H); MS(ES-API) *m/z*:408.1 (M+1); yield: 59.6%; m.p. 107-109 ^{O}C.

ethyl (Z)-3-(2-(2-(2-ethoxy-2-oxoethylidene)-4-oxothiazolidin-3-yl)ethoxy)benzoate (compound 7b)

^{1}H-NMR($CDCl_3$, 400MHz): δ: 7.68 (d, 2H, J = 8.0 Hz), 7.51 (d, 2H, J = 8.0 Hz), 7.34 (t, 1H, J = 7.2 Hz), 7.04 (s, 1H), 5.71 (s, 1H), 4.35 (q, 2H, J = 7.0 Hz), 4.24 (t, 2H, J = 5.4 Hz), 4.21

(q, 2H, *J* = 7.0 Hz), 4.11 (t, 2H, *J* = 4.0 Hz), 3.74 (s, 2H), 1.29-1.38 (m, 6H); MS(ES-API) *m/z*: 380.2 (M+1); yield: 57.3%; m.p. 108-110 ^{O}C.

ethyl (Z)-3-(4-(2-(2-ethoxy-2-oxoethylidene)-4-oxothiazolidin-3-yl)butoxy)benzoate (compound 7c)

^{1}H-NMR($CDCl_3$, 400MHz): *δ*: 7.57 (dt, 1H, *J* = 7.6 Hz, *J* = 1.2 Hz), 7.47 (t, 1H, *J* = 2.0 Hz), 7.27 (t, 1H, *J* = 8.0 Hz), 7.02 (ddd, 1H, *J* = 8.0 Hz, *J* =2.8 Hz, , *J* =0.8 Hz), 5.47(s, 1H), 4.31 (q, 2H, *J* = 7.2 Hz), 4.17 (q, 2H, *J* = 8.2 Hz), 4.00 (s, 2H), 3.69 (t, 2H, *J* = 6.8 Hz), 3.65 (s, 2H), 1.77 (t, 3H, *J* = 6.4 Hz), 1.48 (s, 1H), 1.32 (t, 2H, *J* = 7.2 Hz), 1.23 (t, 2H, *J* = 7.2 Hz); MS(ES-API) *m/z*: 425.2(M+H_2O); yield: 51.9%; m.p. 82-84 ^{O}C.

ethyl(Z)-2-(3-(2-(4-(2-ethoxy-2-oxoethyl)phenoxy)ethyl)-4-oxothiazolidin-2-ylidene)acetate (compound 7d)

^{1}H-NMR($CDCl_3$, 400MHz):*δ*: 7.19 (d, 2H, *J* = 1.2 Hz), 6.81 (d, 2H, *J* = 1.2 Hz), 5.73 (s, 1H), 4.25 (q, 2H, *J* = 7.2 Hz), 4.13-4.23 (m, 6H), 4.08 (t, 1H, *J* = 7.2 Hz), 3.74 (s, 2H), 1.32 (t, 3H, *J* = 7.2 Hz), 1.26 (t, 3H, *J* = 7.2 Hz); MS(ES-API) *m/z*: 394.1 (M+1); yield: 47%; m.p. 93-95 ^{O}C.

ethyl(Z)-2-(3-(4-(4-(2-ethoxy-2-oxoethyl)phenoxy)butyl)-4-oxothiazolidin-2-ylidene)acetate (compound 7e)

^{1}H-NMR($CDCl_3$, 400MHz): *δ*: 7.99 (d, 2H, *J* = 8.0 Hz), 6.91 (d, 2H, *J* = 7.2 Hz), 5.54 (s, 1H), 4.35 (q, 2H, *J* = 7.2 Hz), 4.22 (q, 2H, *J* = 7.2 Hz), 4.25 (t, 2H, *J* = 5.2 Hz), 3.71-3.78 (m, 4H), 1.84 (t, 4H, *J* = 3.2 Hz), 1.38 (t, 3H, *J* = 7.2 Hz), 1.30 (t, 3H, *J* = 6.8 Hz), 1.25 (t, 1H, *J* = 7.2 Hz); MS(ES-API) *m/z*: 422.2 (M+1); 423.1(M+2); 439.2(M+H_2O); yield: 40.1%; m.p. 85-87 ^{O}C.

ethyl (Z)-2-(3-(2-(2-nitrophenoxy)ethyl)-4-oxothiazolidin-2-ylidene)acetate (compound 7f)

^{1}H-NMR($CDCl_3$, 400MHz): δ: 7.83 (dd, 1H, J = 8.0 Hz, J = 1.6 Hz), 7.61-7.66 (m, 1H), δ: 7.83 (dd, 1H, J = 8.4 Hz, J = 0.8 Hz), 7.12 (t, 1H, J = 8.2 Hz), 5.76(s, 1H), 4.33 (t, 2H, J = 5.2 Hz), 4.09-4.11 (m, 4H), 3.83 (s, 2H), 1.20 (t, 3H, J = 8.2 Hz); MS(ES-API) *m/z*: 353.1 (M+1); yield: 40.6%; m.p. 154-156 ^{O}C.

ethyl (Z)-2-(3-(4-(4-nitrophenoxy)butyl)-4-oxothiazolidin-2-ylidene)acetate
(compound 7g)

^{1}H-NMR($CDCl_3$, 400MHz): δ: 8.21 (d, 1H, J = 9.2 Hz), 6.95 (d, 1H, J = 9.2 Hz), 4.22 (q, 2H, J = 7.2 Hz), 4.10 (t, 1H, J = 5.6 Hz), 3.77 (t, 1H, J = 6.8 Hz), 3.72 (s, 2H), 1.83-1.87 (m, 4H), 1.30 (t, 3H, J = 7.2 Hz); MS(ES-API) *m/z*: 398.2(M+H_2O); yield: 57.8%; m.p. 142-144 ^{O}C.

ethyl (Z)-2-(3-(2-(4-nitrophenoxy)ethyl)-4-oxothiazolidin-2-ylidene)acetate
(compound 7h)

^{1}H-NMR($CDCl_3$, 400MHz): δ: 8.20 (d, 2H, J = 9.6 Hz), 7.09 (d, 2H, J = 9.2 Hz), 5.82 (s, 1H), 4.30 (t, 2H, J = 5.2 Hz), 4.09-4.13 (m, 4H), 3.88 (s, 2H), 3.34 (s, 2H), 1.21 (t, 2H, J = 7.2 Hz); MS(ES-API) *m/z*: 353.1 (M+1); 370.1(M+H_2O); yield: 52.1%; m.p. 161-164 ^{O}C.

The analysis of binding and selectivity for inhibitor compound 7d

Of the eight derivatives, the compound 7d ranked the first in the initial molecular docking simulations and showed the most potent inhibitory activity and significant selectivity for PTP-LAR with the IC_{50} value at 10.41 μM over PTP1B(44.40 μM) (Table 2), and hence it was singled out for further investigation. The results of receptor–ligand interactions obtained from the docking simulation had proved that the key residues for the binding interactions between compound 7d and the receptor were fully consistent with the previous reports (Figure 2). The compound 7d is found in the PTP-LAR active-site pocket and forms extensive interactions with residues in the pTyr recognition loop (residues 1352-1355), WPD-loop (residues 1488-1490), P-loop (residues 1521-1528). The O24 atom of compound 7d makes two hydrogen bonds with the main chain amides Trp1488 of WPD-loop and Gln1570;

The O6 atom and O15 of compound 7d also forms two hydrogen bonds with Lys1433; The O23 atom interacts with residue Gln1566 via a strong H-bond. A number of H-bonds significantly enhance the enzyme–inhibitor interaction and stabilize the PTP-LAR–4-thiazolidone derivatives complex within the active site to a great extent. In addition to the polar interactions, the benzene ring group of compound 7d participates in hydrophobic interactions with Ser 1523 in the P-loop. The C12 atom of compound 7d is engaged in alkyl hydrophobic interaction with Tyr1563. The 2D diagram of PTP-LAR-compound 7d, interactions were shown in Figure 3, pink plates such as Asn1357, Lys1433,Trp1488, Gly1492, Ser1523, Arg1528, Gln1566, and Gln1570,were involved in hydrogen bonding, charge or polar interactions, while green plates likeTyr1355, Val 1358, Glu1428, Asp1490, Val1493,Cys1522, Ala1524, Gly1527, Tyr1563, and Thr1567, and Asp1569 represented van der waals interactions. Interestingly, Asn1357 and Tyr 1563 are unique to PTP-LAR, which means no other PTPs have the same amino acids at the corresponding positions. It is likely that the van der waals interaction between the tail of Ar of group is responsible for the potency and selectivity of compound 7d. The tail of Ar of inhibitors is buried well in the site B as shown by the red-white-blue surface in Figure 2. Compared with other compounds designed, the compound 7d has increased polarity fragment, which is more fitted to the second binding site, resulting in the much better binding affinity than any other compounds. Collectively, the structural observations offer direct evidence that compound 7d achieves its potency and specificity for PTP-LAR by targeting unique nearby peripheral binding pockets as well as the active site.

Table 2: 4-thiazolidone derivatives targeting PTP-LAR inhibitors

Cpds	CDOCKER (-Kcal/moL)				IC_{50} (μM)			
	PTP-LAR	PTP1B	SHP2	CDC25B	PTP-LAR	PTP1B	SHP2	CDC25B
7a	27.86	20.91	15.94	15.33	26.05	42.90	>118.72	>118.72

7b	30.63	17.74	10.47	10.12	24.10	46.12	>131.54	>131.54
7c	37.65	16.11	9.86	10.05	14.38	98.2	>131.89	>131.89
7d	39.44	19.14	14.66	13.86	10.41	44.40	>122.81	>122.81
7e	36.63	21.56	13.58	12.95	11.08	31.60	>122.81	>122.81
7f	21.34	16.32	12.45	12.62	27.28	81.7	>122.81	>122.81
7g	33.79	17.49	11.49	11.78	13.07	72.20	>126.86	>126.86
7h	23.40	16.02	9.52	9.83	25.40	105.3	>131.58	>131.58
ZINC33404314	20.56	14.06	8.23	8.05	-	-	-	-

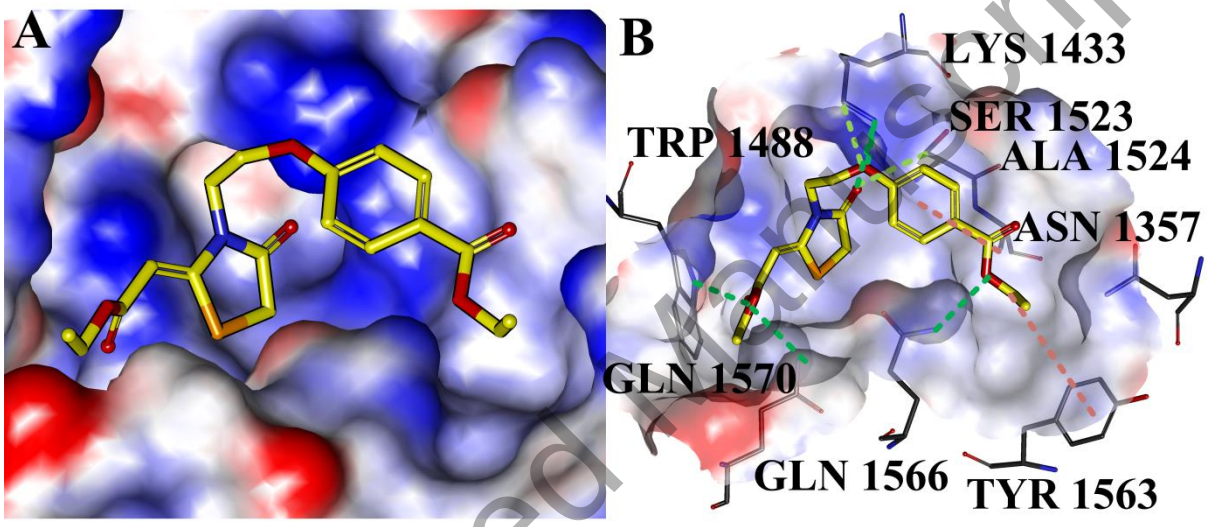

Figure 2 Interaction of the receptor with the docked compound 7d. (A) The molecular surface is shown around the binding site of 1LAR (B) The green dotted lines indicate the H-bond interactions of the receptor with compound 7d; The pink dotted lines indicate the hydrophobic interactions of the receptor with compound 7d.

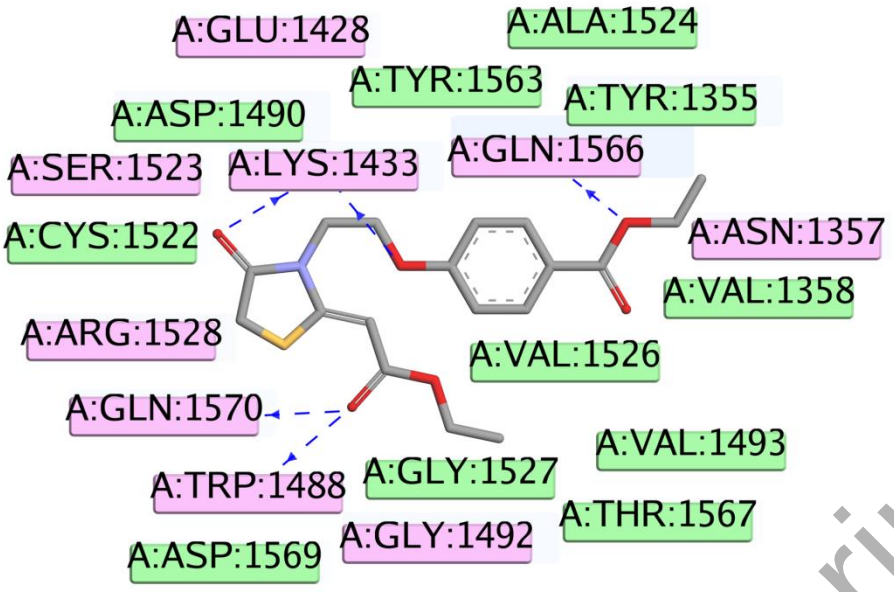

Figure 3 The 2D diagram of PTP-LAR-compound 7d. Residues involved in hydrogen-bond, charge or polar interactions are represented by pink boxes. Residues involved in van der waals interactions are represented by green boxes. Hydrogen-bond interactions with amino acid main chains and side chains are represented by a green and blue dashed arrow directed towards the electron donor.

Molecular Dynamics Trajectory Analysis

In order to acquire the relevant information for characterizing the internal motions of biomacromolecules with time, the 50 ns molecular dynamic simulations were carried out, respectively, for the crystal structures of PTP-LAR(1LAR), the complexes with compound 7d: PTP-LAR–compound 7d, and the complexes with compound 7f: PTP-LAR–compound 7f. The corresponding root mean square deviation (RMSD) from the initial conformation is a major criterion used to evaluate the stability of a protein system. The RMSD value curves of the protein backbone for PTP-LAR, PTP-LAR–compound 7d and PTP-LAR–compound 7f were computed, respectively. As we can see from Figure 4, all of the characters concerned reached the simulation equilibrium within the 2 ns. During the simulation, the RMSD of PTP-

LAR for both the complexes with ligand compound 7d and compound 7f was found to be relatively stable about 0.5 Å and 0.7 Å, respectively. Interestingly, the RMSD value of both PTP-LAR–compound 7d and PTP-LAR–compound 7f is smaller than that of PTP-LAR, indicating that the complexes of PTP-LAR–compound 7d and PTP-LAR–compound 7f are more stable than PTP-LAR, particularly for the case of PTP-LAR–compound 7d system.

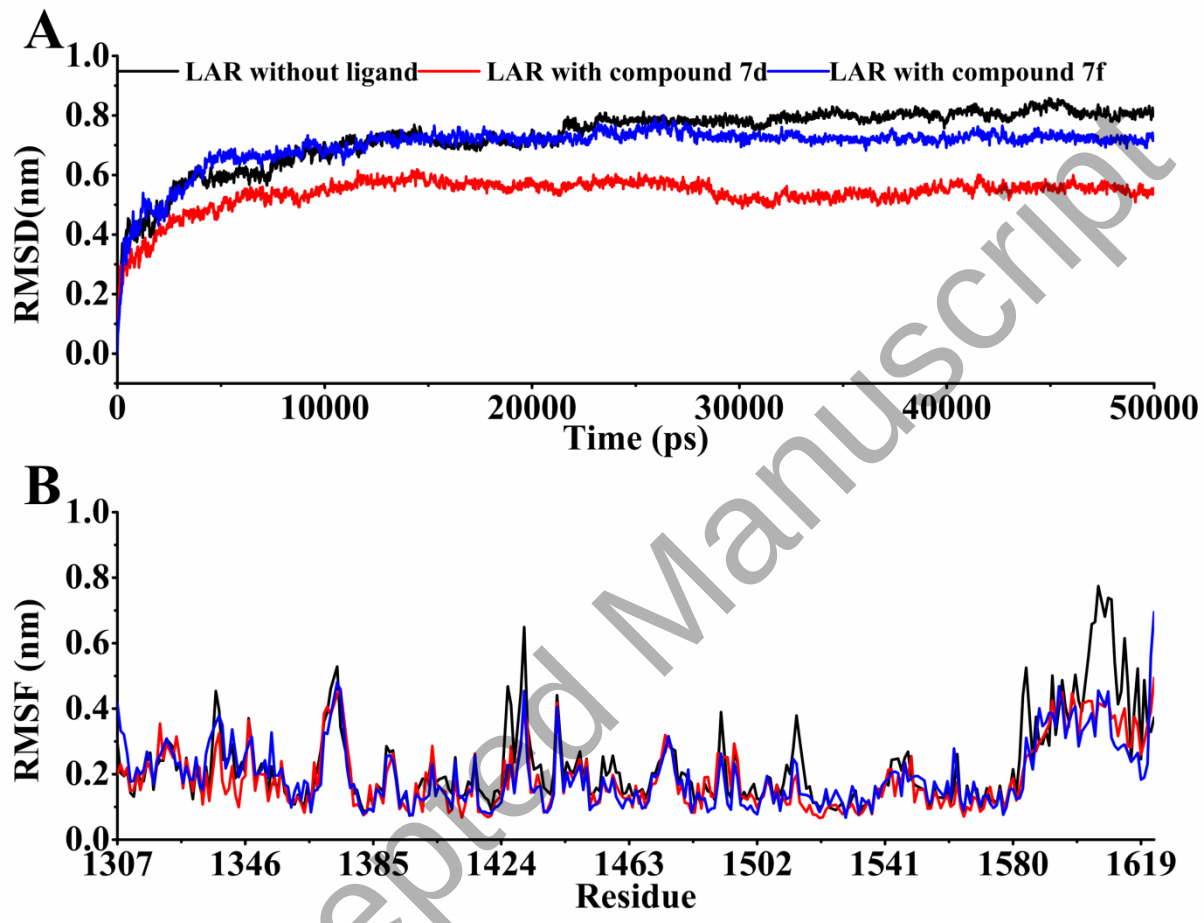

Figure 4 Illustration to show the outcomes of molecular dynamics simulations for compound 7d and compound 7f. (A) The RMSD (root mean square deviation) of all backbone atoms for the receptor PTP-LAR. (B) The RMSF (root mean square fluctuation) of the side-chain atoms for the receptor PTP-LAR. The black line indicates the outcome for the system of the receptor alone without any ligand, the red line for that of the receptor with the ligand compound 7d, the blue line for that of the receptor with the ligand compound 7f.

To perform an in-depth study of the interactions of the PTP-LAR binding domain with

the inhibitor, the root mean square fluctuations for all the side-chain atoms of the receptors were also computed within 50 ns molecular dynamics simulations, as shown in panel B of Figure 4. The RMSF fluctuated large, which meant the residues were unstable, whereas the RMSF fluctuated small, which meant the residues were stable. In the active site-pTyr recognition loop (residues 1352-1355), the order of the RMSF values was compound 7d<protein without compound< compound 7f, indicating that compound 7d could inhibit the fluctuations in the pTyr recognition loop and compound 7f could not did that. In the WPD-loop (residues 1488-1490), the order of the RMSF values was compound 7d≈compound 7f <without compound, showing that both compound 7d and compound 7f could inhibit the fluctuations in the WPD-loop. In P-loop (residues 1521-1528), the order of the RMSF values was compound 7d < without compound ≈ compound 7f, meant that compound 7d could inhibit the fluctuations in the P-loop, while compound 7f could not. unique binding site-residues Asn1357 and Tyr 1563, both compound 7d and compound 7f had lower the RMSF values than protein without compound, showing that both compound 7d and compound 7f could inhibit the unique area. It can be seen from the figure that the side-chain of the root mean square fluctuations of the complexes of PTP-LAR–compound 7d was lower than PTP-LAR. This is particularly true for in the active site-pTyr recognition loop (residues 1352-1355), WPD-loop (residues 1488-1490), P-loop (residues 1521-1528) and unique binding site- residues Asn1357 and Tyr 1563, suggesting an overall more rigid and stable structure for PTP-LAR–compound 7d identified in the present study.

MM-PBSA method was applied to calculate components of binding energy(Kumari, Kumar, Open Source Drug Discovery & Lynn 2014). The MM/PBSA approach was composed of four terms, i.e., the Van der Waals interaction energy, the electrostatic energy, the polar solvation free energy, and the non-polar solvation free energy. Van der Waals, electrostatic interactions and non-polar solvation energy made a negative contribution to the total interaction energy while only polar solvation energy made a positive contribution to the total free binding energy, which meant that Van der Waals, electrostatic interactions and non-polar solvation energy together are in favor of the stability of the complex system. The

binding energy of compound 7d with PTP-LAR is -184.245 kcal/mol, while the binding energy of compound 7f with PTP-LAR is -85.618 kcal/mol, indicating that the system of PTP-LAR - compound 7d seems more stable than PTP-LAR-compound 7f(Table 3), which was in accord with the bioactivity results. We could clearly see that the Van der Waal interactions and the electrostatic interactions were the major favorable contributions to the binding energies between PTP-LAR and compound 7d/ compound 7f. Consistent with the results of molecular docking (Figure 3 and Figure S2), Van der Waals interactions and the electrostatic interactions played the main role in both PTP-LAR/compound 7d and PTP-LAR/compound 7f system.

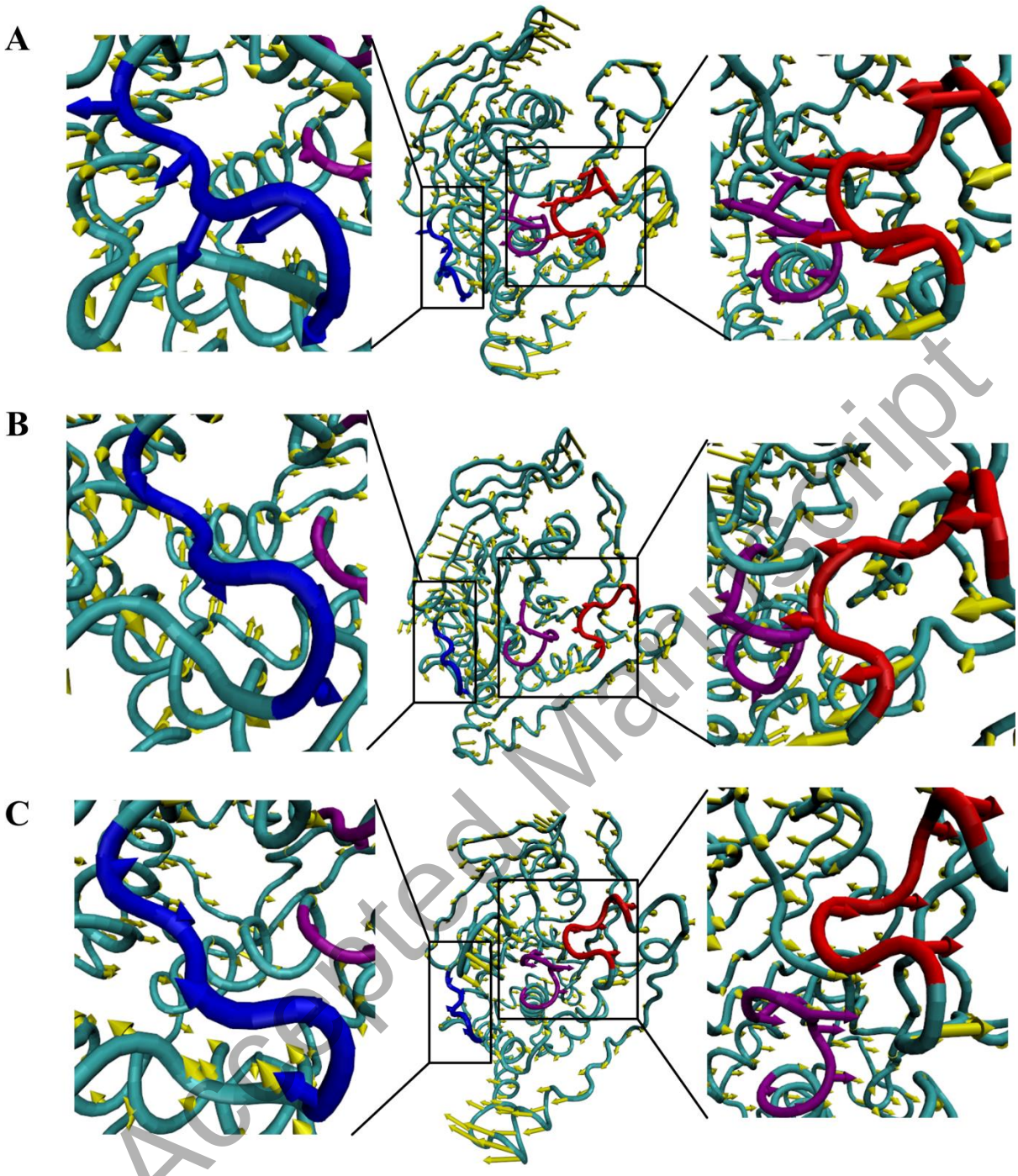

Figure 5. (A) The ANM analysis of PTP-LAR system, (B) The ANM analysis of PTP-LAR-compound7d system, (C) The ANM analysis of PTP-LAR-compound7f system.The length of arrows is positively-correlated with motive magnitude, and the orientation of arrow indicates motive direction. The pTyr recognition loop (residues 1352-1355) , WPD-loop (residues 1488-1490) and P-loop (residues 1521-1528) are marked in red, blue, and purple,

respectively. The areas (pTyr recognition loop,WPD-loop,and P-loop) are magnified and present on the right side of the picture.

Table 3 Binding free energies (kcal/mol) and its components between receptor and ligand, respectively.

complex	Van der Waal (Kcal/mol)	Electrostatic (Kcal/mol)	Polar solvation (Kcal/mol)	Non-polar solvation (Kcal/mol)	Binding energy (Kcal/mol)
LAR-compound 7d	-151.077	-164.314	145.352	-14.206	-184.245
LAR-compound 7f	-167.993	-153.364	250.435	-14.696	-85.618

In order to clearly discern the contributions of binding free energy of each residue, the interaction energies are decomposed into individual residue contributions using energy decomposition scheme(Baker, Sept, Joseph, Holst & McCammon 2001). The residues with the top 10 interaction energies for compound 7d with PTP-LAR, respectively, are shown in Figure 6. The binding energy is defined as the sum of short range electrostatic interactions and van der Waals interactions between the receptor and the ligand. The key residues were observed in four significantly different regions the active site-pTyr recognition loop (residues 1352-1355), WPD-loop (residues 1488-1490), P-loop (residues 1521-1528) and unique binding site- residues Asn1357 and Tyr 1563 of PTP-LAR, which was in accordance with the RMSF results in Figure 4.For PTP-LAR-compound 7d binding system, the residues Val1526, Lys1433, Tyr1563, Val1358, and Tyr1355 made large contributions to the binding affinity. Their total energy contributions are -4.52 kcal/mol,-3.22 kcal/mol, -2.53 kcal/mol, -1.96 kcal/mol, and -1.71 kcal/mol, respectively. As shown in Figure6, V1526 in P-loop makes remarkable contributions to the binding affinity, its contribution to total energy is -4.52 kcal/mol, which explained why compound 7d showed good activities. In addition, the contributions of the residues in site B which are relate to the selectivity of PTP-LAR are -2.54 kcal/mol (Tyr1563), -1.55 kcal/mol (Asn1357), accounting for the high selectivity of

compound 7d. Figure 5 also revealed the compound 7f had the same binding residues as compound 7d but had lower binding affinity, explaining that compound 7f had less bioactivity than compound 7d.

In a word, all of these are very important reasons to explain the high activity and selectivity of compound 7d for PTP-LAR.

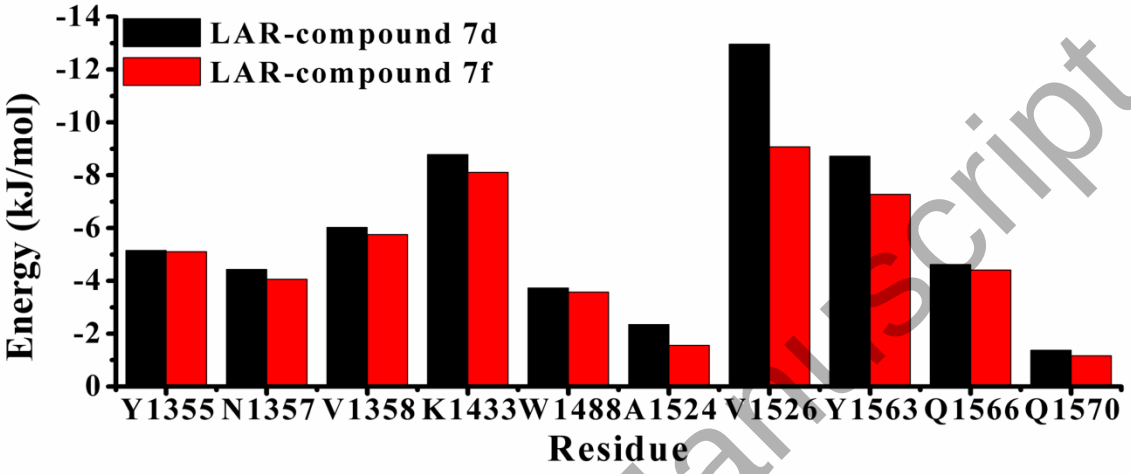

Figure 6 The top ten pairwise residue interaction energies of PTP-LAR/compound7d (black) and PTP-LAR/compound7f complex (red).

Conclusion

The goal of this study was to discover novel and potential selective PTP-LAR inhibitors. Fragment replace was applied in this study to help lengthen the 4-thiazolidone ring structure to make it better fit the roomy space in site B to improve selectivity. It was further validated by the outcomes of their ADME predictions that the hits hold high potential to become drug candidates. The eight compounds have the capable of inhibiting PTP-LAR. It is interesting to discover that compound7d showed highly selectivity for PTP-LAR (10.41 μM) over its close homolog PTP1B (IC_{50}=44.40 μM), SHP2 (IC_{50}>122.81 μM) and CDC25B (IC_{50}>122.81 μM). Through molecular docking and molecular dynamic studies, a most likely binding mode was

proposed, suggesting that the potency and selectivity of the PTP-LAR inhibitors could be achieved by targeting peripheral pockets and the active site.

Acknowledgments

This study was supported by the National Natural Science Foundation of China (Grant No. 81773569), the Natural Science Foundation of Tianjin (Grant No. 18JCQNJC13700), the Cooperation and Exchange Project of the National Natural Science Foundation of China (Grant No.81611130090), the Science & Technology Development Fund of Tianjin Education Commission for Higher Education (Grant No. 2017KJ229).

Conflict of interest

There is no conflict of interest.

Supplemental material

Figure S1 Relationship between the experimental pIC_{50} and the docking score of 20 inhibitors of PTP-LAR (R^2=0.93).

Figure S2 The 2D diagram of PTP-LAR-compound 7f.

Figure S3 The docked poses of 20 inhibitors of PTP-LAR.

Reference

Ahmad, F. & Goldstein, B. J. (1997). Functional association between the insulin receptor and the transmembrane protein-tyrosine phosphatase LAR in intact cells. *J Biol Chem 272*: 448-457.

Ajay, D. & Sobhia, M. E. (2012). Identification of novel, less toxic PTP-LAR inhibitors using in silico strategies: pharmacophore modeling, SADMET-based virtual screening and docking. *Journal of molecular modeling 18*: 187-201.

Andrew S., S. D. K., Steven L. T. (1995). Analysis of Conformational Coverage. 1. Validation and Estimation of Coverage. *Journal of Chemical Information and*

Computer Sciences 35: 285-294.

Andrew S., S. D. K., Steven L. T. (1995). Analysis of Conformational Coverage. 2. Applications of Conformational Models. *Journal of Chemical Information and Computer Sciences 35*.

Andrew S., S. L. T., Peter T. (1995). Poling: Promoting Conformational Variation. *Journal of Computational Chemistry 16*: 171-187.

Baker, N. A., Sept, D., Joseph, S., Holst, M. J. & McCammon, J. A. (2001). Electrostatics of nanosystems: application to microtubules and the ribosome. *Proc Natl Acad Sci U S A 98*: 10037-10041.

Berman, H. M., Battistuz, T., Bhat, T. N., Bluhm, W. F., Bourne, P. E., Burkhardt, K., Feng, Z., Gilliland, G. L., Iype, L., Jain, S., Fagan, P., Marvin, J., Padilla, D., Ravichandran, V., Schneider, B., Thanki, N., Weissig, H., Westbrook, J. D. & Zardecki, C. (2002). The Protein Data Bank. *Acta Crystallogr D Biol Crystallogr 58*: 899-907.

Chagnon, M. J., Uetani, N. & Tremblay, M. L. (2004). Functional significance of the LAR receptor protein tyrosine phosphatase family in development and diseases. *Biochemistry and Cell Biology-Biochimie Et Biologie Cellulaire 82*: 664-675.

Chagnon, M. J., Uetani, N. & Tremblay, M. L. (2004). Functional significance of the LAR receptor protein tyrosine phosphatase family in development and diseases. *Biochemistry and Cell Biology 82*: 664-675.

Cheng, A. & Dixon, S. L. (2003). In silico models for the prediction of dose-dependent human hepatotoxicity. *J Comput Aided Mol Des 17*: 811-823.

Cheng, A. & Merz, K. M., Jr. (2003). Prediction of aqueous solubility of a diverse set of compounds using quantitative structure-property relationships. *Journal of Medicinal Chemistry 46*: 3572-3580.

Dixon, S. L. & Merz, K. M., Jr. (2001). One-dimensional molecular representations and similarity calculations: methodology and validation. *Journal of Medicinal Chemistry 44*: 3795-3809.

Egan, W. J. & Lauri, G. (2002). Prediction of intestinal permeability. *Adv Drug Deliv Rev 54*:

273-289.

Egan, W. J., Merz, K. M., Jr. & Baldwin, J. J. (2000). Prediction of drug absorption using multivariate statistics. *Journal of Medicinal Chemistry 43*: 3867-3877.

Egan, W. J., Walters, W. P. & Murcko, M. A. (2002). Guiding molecules towards drug-likeness. *Curr Opin Drug Discov Devel 5*: 540-549.

Elchebly, M., Cheng, A. & Tremblay, M. L. (2000). Modulation of insulin signaling by protein tyrosine phosphatases. *J Mol Med (Berl) 78*: 473-482.

Ftanik, J. & Horvath, I. I. (1989). Computations of energy levels and wave functions of ground and excited states by the steepest-descent method. *Phys Rev D Part Fields 40*: 642-649.

Guan, K. L. & Dixon, J. E. (1991). Evidence for protein-tyrosine-phosphatase catalysis proceeding via a cysteine-phosphate intermediate. *J Biol Chem 266*: 17026-17030.

Hashimoto, N., Feener, E. P., Zhang, W. R. & Goldstein, B. J. (1992). Insulin receptor protein-tyrosine phosphatases. Leukocyte common antigen-related phosphatase rapidly deactivates the insulin receptor kinase by preferential dephosphorylation of the receptor regulatory domain. *J Biol Chem 267*: 13811-13814.

Hess, B. (2008). P-LINCS: A Parallel Linear Constraint Solver for Molecular Simulation. *J Chem Theory Comput 4*: 116-122.

Hess, B., Kutzner, C., van der Spoel, D. & Lindahl, E. (2008). GROMACS 4: Algorithms for Highly Efficient, Load-Balanced, and Scalable Molecular Simulation. *J Chem Theory Comput 4*: 435-447.

Irwin, J. J. & Shoichet, B. K. (2005). ZINC--a free database of commercially available compounds for virtual screening. *J Chem Inf Model 45*: 177-182.

Konerding, D. E., Cheatham, T. E., 3rd, Kollman, P. A. & James, T. L. (1999). Restrained molecular dynamics of solvated duplex DNA using the particle mesh Ewald method. *Journal of Biomolecular Nmr 13*: 119-131.

Kulas, D. T., Zhang, W. R., Goldstein, B. J., Furlanetto, R. W. & Mooney, R. A. (1995). Insulin receptor signaling is augmented by antisense inhibition of the protein tyrosine

phosphatase LAR. *J Biol Chem 270*: 2435-2438.

Kumari, R., Kumar, R., Open Source Drug Discovery, C. & Lynn, A. (2014). g_mmpbsa--a GROMACS tool for high-throughput MM-PBSA calculations. *J Chem Inf Model 54*: 1951-1962.

Lipinski, C. A. (2016). Rule of five in 2015 and beyond: Target and ligand structural limitations, ligand chemistry structure and drug discovery project decisions. *Adv Drug Deliv Rev 101*: 34-41.

Lipinski, C. A., Lombardo, F., Dominy, B. W. & Feeney, P. J. (2001). Experimental and computational approaches to estimate solubility and permeability in drug discovery and development settings. *Adv Drug Deliv Rev 46*: 3-26.

Lombardo, F., Gifford, E. & Shalaeva, M. Y. (2003). In silico ADME prediction: data, models, facts and myths. *Mini Reviews in Medicinal Chemistry 3*: 861-875.

MacKerell, A. D., Banavali, N. & Foloppe, N. (2001). Development and current status of the CHARMM force field for nucleic acids. *Biopolymers 56*: 257-265.

Markovic, R., Baranac, M., Dzambaski, Z., Stojanovic, M. & Steel, P. J. (2003). High regioselectivity in the heterocyclization of beta-oxonitriles to 4-oxothiazolidines: X-ray structure proof. *Tetrahedron 59*: 7803-7810.

Markovic, R., Pergal, M. M., Baranac, M., Stanisavljev, D. & Stojanovic, M. (2006). An expedient solvent-free synthesis of (Z)-2-alkylidene-4-oxothiazolidine derivatives under microwave irradiation. *Arkivoc*: 83-90.

Mediavilla Bravo, J. J. (2014). [Guidelines for the management of diabetes mellitus type 2]. *Semergen 40 Suppl 4*: 11-18.

Michigan Dental, A. (2007). Patient fact sheet. Diabetes and your oral health. *J Mich Dent Assoc 89*: 17.

Nam, H. J., Poy, F., Krueger, N. X., Saito, H. & Frederick, C. A. (1999). Crystal structure of the tandem phosphatase domains of RPTP LAR. *Cell 97*: 449-457.

Norberto de Souza, O. & Ornstein, R. L. (1999). Molecular dynamics simulations of a protein-protein dimer: particle-mesh Ewald electrostatic model yields far superior

results to standard cutoff model. *Journal of Biomolecular Structure & Dynamics 16*: 1205-1218.

Pol-Fachin, L., Fernandes, C. L. & Verli, H. (2009). GROMOS96 43a1 performance on the characterization of glycoprotein conformational ensembles through molecular dynamics simulations. *Carbohydr Res 344*: 491-500.

Premnath, P. N., Liu, S., Perkins, T., Abbott, J., Anderson, E. & McInnes, C. (2014). Fragment based discovery of arginine isosteres through REPLACE: Towards non-ATP competitive CDK inhibitors. *Bioorganic & Medicinal Chemistry 22*: 616-622.

Pulido, R., Serra-Pages, C., Tang, M. & Streuli, M. (1995). The LAR/PTP delta/PTP sigma subfamily of transmembrane protein-tyrosine-phosphatases: multiple human LAR, PTP delta, and PTP sigma isoforms are expressed in a tissue-specific manner and associate with the LAR-interacting protein LIP.1. *Proc Natl Acad Sci U S A 92*: 11686-11690.

Rathmann, W. & Giani, G. (2004). Global prevalence of diabetes: estimates for the year 2000 and projections for 2030. *Diabetes Care 27*: 2568-2569; author reply 2569.

Ren, J. M., Li, P. M., Zhang, W. R., Sweet, L. J., Cline, G., Shulman, G. I., Livingston, J. N. & Goldstein, B. J. (1998). Transgenic mice deficient in the LAR protein-tyrosine phosphatase exhibit profound defects in glucose homeostasis. *Diabetes 47*: 493-497.

Roper, D., Spinderella, D. J. & Webb, R. (2014). Let's talk about ... diabetes. *Diabetes Forecast 67*: 50-53.

Susnow, R. G. & Dixon, S. L. (2003). Use of robust classification techniques for the prediction of human cytochrome P450 2D6 inhibition. *J Chem Inf Comput Sci 43*: 1308-1315.

Tsujikawa, K., Kawakami, N., Uchino, Y., Ichijo, T., Furukawa, T., Saito, H. & Yamamoto, H. (2001). Distinct functions of the two protein tyrosine phosphatase domains of LAR (leukocyte common antigen-related) on tyrosine dephosphorylation of insulin receptor. *Molecular Endocrinology 15*: 271-280.

van Aalten, D. M., Bywater, R., Findlay, J. B., Hendlich, M., Hooft, R. W. & Vriend, G.

(1996). PRODRG, a program for generating molecular topologies and unique molecular descriptors from coordinates of small molecules. *J Comput Aided Mol Des 10*: 255-262.

Viswanathan, V. & Sathyamurthy, S. (2015). Global Increase in the Prevalence of Diabetes with Special Reference to the Middle East and Asia. *Diabetes Technol Ther 17*: 676-678.

Votano, J. R., Parham, M., Hall, L. M., Hall, L. H., Kier, L. B., Oloff, S. & Tropsha, A. (2006). QSAR modeling of human serum protein binding with several modeling techniques utilizing structure-information representation. *Journal of Medicinal Chemistry 49*: 7169-7181.

Walters, W. P. (2012). Going further than Lipinski's rule in drug design. *Expert Opin Drug Discov 7*: 99-107.

Wesson, L. & Eisenberg, D. (1992). Atomic solvation parameters applied to molecular dynamics of proteins in solution. *Protein Sci 1*: 227-235.

Wild, S., Roglic, G., Green, A., Sicree, R. & King, H. (2004). Global prevalence of diabetes: estimates for the year 2000 and projections for 2030. *Diabetes Care 27*: 1047-1053.

Wu, J.-w., Yin, L., Liu, Y.-q., Zhang, H., Xie, Y.-f., Wang, R.-l. & Zhao, G.-l. (2019). Synthesis, biological evaluation and 3D-QSAR studies of 1, 2, 4-triazole-5-substituted carboxylic acid bioisosteres as uric acid transporter 1 (URAT1) inhibitors for the treatment of hyperuricemia associated with gout. *Bioorganic & Medicinal Chemistry Letters 29*: 383-388.

Wu, J., Sun, Y., Zhou, H., Ma, Y. & Wang, R. (2019). Design, synthesis, biological evaluation and molecular dynamics simulation studies of (R)-5-methylthiazolidin-4-One derivatives as megakaryocyte protein tyrosine phosphatase 2 (PTP-MEG2) inhibitors for the treatment of type 2 diabetes. *Journal of Biomolecular Structure and Dynamics*: 1-10.

Xia, X., Maliski, E. G., Gallant, P. & Rogers, D. (2004). Classification of kinase inhibitors using a Bayesian model. *Journal of Medicinal Chemistry 47*: 4463-4470.

Xu, E., Schwab, M. & Marette, A. (2014). Role of protein tyrosine phosphatases in the modulation of insulin signaling and their implication in the pathogenesis of obesity-linked insulin resistance. *Rev Endocr Metab Disord 15*: 79-97.

Zabolotny, J. M., Kim, Y. B., Peroni, O. D., Kim, J. K., Pani, M. A., Boss, O., Klaman, L. D., Kamatkar, S., Shulman, G. I., Kahn, B. B. & Neel, B. G. (2001). Overexpression of the LAR (leukocyte antigen-related) protein-tyrosine phosphatase in muscle causes insulin resistance. *Proc Natl Acad Sci U S A 98*: 5187-5192.

Zhang, W. R., Li, P. M., Oswald, M. A. & Goldstein, B. J. (1996). Modulation of insulin signal transduction by eutopic overexpression of the receptor-type protein-tyrosine phosphatase LAR. *Molecular Endocrinology 10*: 575-584.

Zhu, Y. & Zhang, C. (2016). Prevalence of Gestational Diabetes and Risk of Progression to Type 2 Diabetes: a Global Perspective. *Curr Diab Rep 16*: 7.